Archives of Advances in Biosciences

Original Article:

Cellular Imaging and Uptake Studies of PEG-coated SPION in Human Derived Endometrium Mesenchymal Stem Cell

Nahid Aboutaleb[۱،۲], **Mahdieh Mehrab Mohseni**[۳], **Maryam Naseroleslami**[۳*], **Ghazal Yousefi**[٤]

۱. Physiology Research Center, Iran University of Medical Sciences, Tehran, Iran.
۲. Department of Physiology, Iran University of Medical Sciences, Tehran, Iran.
۳. Department of Cellular and Molecular Biology, Faculty of Advanced Science and Technology, Tehran Medical Sciences, Islamic Azad University, Tehran, Iran.
٤. Department of Veterinary Medicine, Science and Research Branch, Islamic Azad University, Tehran, Iran.

Cite this article as: Aboutaleb N, Mehrab Mohseni M, Naseroleslami M, Yousefi Gh. Cellular Imaging and Uptake Studies of PEG-coated SPION in Human Derived Endometrium Mesenchymal Stem Cell. Archives of Advances in Biosciences. ۲۰۲۳; ۱٤:E۳۹۷۷۷. https://doi.org/۱۰,۲۲۰۳۷/aab.v۱٤i۱,۳۹۷۷۷

https://journals.sbmu.ac.ir/aab/article/view/۳۹۷۷۷

Article info:
Received: ۲۰ Oct ۲۰۲۲
Accepted: ۲۹ Dec ۲۰۲۲
Published: ۲۲ May ۲۰۲۳

*** Corresponding author:**

Maryam Naseroleslami, PhD.

Address: Department of Cellular and Molecular Biology, Faculty of Advanced Science and Technology, Tehran Medical Sciences, Islamic Azad University, Tehran, Iran.

E-mail:
naseroleslami@gmail.com

Abstract

Introduction: As human endometrium Mesenchymal stem cells (hEMSCs) therapy has been used to treat different diseases, its tracing is essential. Low image sensitivity is one of the most critical problems. In this study, thus, transplanted hEMSCs were labeled with the PEG-coated SPION nanoparticles for the first time to improve low image sensitivity at Magnetic resonance imaging (MRI) for more efficient in vivo tracking of cells. To achieve the goals, we evaluated the effects of various concentrations of PEG-coated SPION (۲۰nm) incubated with hEMSCs on cytotoxicity and cell survival. PEG-coated SPION uptake into the cytoplasm of hEMSCs was confirmed by Prussian Blue staining ٤۸ and ۷۲h after incubation at ۰, ۱۰۰, ۲۰۰, and ۳۰۰ µg/ml concentrations; the data on the Atomic Absorption Spectroscopy (AAS) confirmed that PEG-coated SPION absorption by hEMSCs increased as much as the dose (P<۰,۰٥). In general, higher concentrations of PEG-coated SPION improved MRI image contrast and enhanced cell fate tracking. Our results suggested that ۱۰۰ µg/ml PEG-coated SPION was ideal because the cytotoxicity was not statically significant compared to that of the control group (p<۰,۰٥). At ۲۰۰ and ۳۰۰ µg/ml concentrations, PEG-coated SPION caused increased oxidative stress and initiated apoptosis and autophagy in hEMSCs. The mechanism of its action was found by evaluation of several key genes; the mRNA levels of apoptosis and autophagy markers, including Bax, Caspase۳, BECLIN, LC۳, and TP٥۳ rose significantly (P<۰,۰٥), while BCL۲ decreased at ۳۰۰ µg/ml concentration (P<۰,۰٥). Therefore, higher concentrations of PEG-coated SPION can increase ROS production in a dose and time-dependent manner.

Keywords: Human endometrium mesenchymal stem cells, Iron nanoparticles, MRI tracking, PEG-coated SPION.

۱. Introduction

The increasing use of stem cells to treat many chronic disorders like various types of cancers and diabetes creates the demand for in vivo cell tracking methods. It is evident that conventional transplanted cells assessment, such as animal and human histologic evaluations, diagnostic antibodies, and staining kits, cannot meet these demands because of their limitations. For example, scarifying the animal models for tissue processing is inevitable [۱-۳]. To overcome this problem, some novel methods with various advantages and disadvantages have been introduced. One of these methods is magnetic resonance imaging (MRI) which is widely used as a non-invasive method with full three-dimensional (۳-D) capabilities, magnificent soft-tissue contrast, and high spatial

resolution. In this method, low sensitivity remains a significant problem. Despite the use of contrast agents in MRI for many years, an ideal contrast agent with low toxicity, a long half-life, and multiple performances is still desirable. Today, Gadolinium chelates are intravenous contrast agents used to enhance vascular structures during diagnostic MRI, and they are widely used to label and track therapeutic cells in preclinical models [١]. However, the sensitivity and safety of Gadolinium raise some concerns. Hence, FDA-approved nanoparticles with biocompatibility that can move towards the magnetic field have been used to track implemented stem cells [٤-٧]. There is evidence that larger particles are more likely to be absorbed by the reticuloendothelial system; therefore, they could be instantly removed from circulation. As smaller particles remain longer in the circulation with more contrast, they can accumulate in the target tissue. This characteristic makes them more desirable for medical uses. Several studies also showed that it is more effective to label stem cells with smaller nanoparticles than larger particles with the same coating [٨-١٠]. Furthermore, nanoparticle coating is also an influential factor, influencing the toxicity, biocompatibility, surface charge, efficiency, and specificity of the nanoparticles [٤, ١١, ١٢].

Coatings can hold different characteristics. For example, hydrophilic coatings like Polyethylene glycol (PEG) prevent the accumulation of nanoparticles and cause them to dissolve. They also do not trigger immune responses [١٣, ١٤].

As choosing the best type of cells is one of the influential factors in cell therapy and regenerative medicine, endometrial mesenchymal stem cells (hEMSCs) have recently been considered as reliable stem cell sources in this research area [٣, ١٥]. This is because of its special advantages like its unique potential for infertility treatment, and not causing autologous graft rejection [١٦]. Based on our previous research, SPION can lead to cell death in some concentrations, but there is no data about its mechanism of action. Thus, in this investigation, we aimed to introduce PEG-coated superparamagnetic iron oxide nanoparticles (SPION) for tracking hEMSCs and evaluate the effects of various concentrations of PEG-coated SPION (٢٠nm) incubated with hEMSCs on cell survival and the mechanism of action of its cytotoxicity for the first time; finding the optimum concentrations with the best function without toxicity will prevent cell damage while providing accurate in vivo tracing of transplanted cells.

٢. Materials and Methods

Nanoparticles Preparation

PEG-coated SPION was synthesized by co-precipitation of ferric salts and ferrous solution via a single-step reaction. This was described in detail in our previous study [٧].

Preparation of cell culture

The stem cells were provided from the Iranian Biological Resource Center, where the cells were obtained from subjects who have already undergone diagnostics endometrial biopsy. All protocols were carried out based on the outlines of the Helsinki Convention and were approved by the research ethics committee of Iran University of medical sciences, Tehran, Iran.

After erythrocyte lysis, cells were suspended in Eagle's Medium (DMEM) and were provided with ١٠٪ fetal bovine se-rum (FBS), $NaHCO^{٣}$ (٣,٧ g/l), penicillin (١٠٠ U/ml), and streptomycin (١٠٠ mg/ml, Sigma, USA); Next, they were grown in the incubators providing ٥٪$CO^{٢}$ at ٣٧°C. Finally, cells were labeled with PEG-coated SPION while the cell line reached about ٧٠-٨٠٪ confluence. Afterward, the culture medium was changed to remove the suspension cells; then, FBS and culture medium were added to the cells attached to the bottom of the flask.

Flow Cytometry

To be sure that the isolated cells were mesenchymal cells, flow cytometry tests were done. In summary, cultured hEMSCs were washed twice in phosphate-buffered saline (PBS), and were then harvested with ٠,٢٥٪ trypsin/EDTA (Invitrogen, USA). The cells were washed with PBS and were divided into several aliquots for specific antibody staining. Each aliquot had nearly ٥×١٠^{٣} cells. The antibodies were against the cell surface antigens: $CD^{٤٥}$, $CD^{٢٩}$, $CD^{٩٠}$, $CD^{٣٤}$, and $CD^{١٠٥}$. All of the mentioned antibodies were conjugated with fluorescein isothiocyanate and phycoerythrin. The cells were stained at ٤°C for ٣٠ minutes. After the incubation period, the cells were washed with PBS and re-suspended in ٥٠٠ µL of PBS. Analysis was performed using flowjo software.

Osteogenic Differentiation

To evaluate the osteogenic differentiation potential of hEMSCs, we incubated them in a ٦-well plate at ٣٧°C, ٥٪ $CO^{٢}$ having ١٠ ml of osteogenic differentiation medium containing ascorbic acid (٥٠

mM) dexamethasone (١٠٠ nM), b-glycerophosphate (١٠ mM) (Sigma-Aldrich, USA), and DMEM+PBS ١٠٪. Basal culture media was changed every ٢-٣ days for three weeks. Basal culture media was used as control. Finally, osteogenic differentiation was evaluated using alizarin red staining.

Alizarin Red Staining

On day ٢١, first, monolayers were washed with PBS; then, they were fixed with ١٠٪ (v/v) neutral-buffered formalin for ١٠ mins, and were fixed in methanol at room temperature for ٣٠ min. After two washes, hEMSCs were stained with Alizarin red solution for ٢٠ min. Then, nonspecific stained cells were rinsed with distilled water, were allowed to dry, and were then evaluated using invert microscopy.

Adipogenic Differentiation

To evaluate the adipogenic differentiation potential of hEMSCs, the third passage of hEMSCs was obtained and cultured at ٣٧°C, ٥٪ CO_2 in differential cell culture media containing DMEM+PBS ١٠٪, dexamethasone (١٠٠ nM), methyl isobutyl xanthine (٠,٥ mM), insulin (١٠ µg/ml), and indomethacin (١٠٠ µM). Basal culture media was used as control. The medium was changed every ٢-٣ days for three weeks. Finally, adipogenic differentiation was detected using Oil Red staining.

Oil Red-O Staining

The cells were fixed through incubation in ٤٪ paraformaldehyde (PFA) for one hour at room temperature and stained in oil red-٠,٥٪ in isopropyl alcohol ٩٩٪ for ١٠-١٥ min. Finally, hEMSCs were washed three times with ٧٠٪ alcohol and were then evaluated with invert microscopy.

hEMSCs incubation with nanoparticles

When the confluency of cells reached about ٧٠٪, cells were treated with iron oxide. The nanoparticles were first sonicated in water (with power and time for ٤ minutes, ٣٠ seconds off, and ٣٠ seconds on). Then, the cells were implanted in culture dishes. After ٢ hours, different concentrations of iron oxide nanoparticles were poured on the cells coated with UV-sterilized polyethylene glycol.

Prussian Blue staining: Evaluating Cellular Uptake nanoparticles

One day after hEMSCs were seeded onto ٦-well plates, they were incubated at concentrations of ٠, ١٠٠, ٢٠٠, and ٣٠٠ µg/ml of iron oxide nanoparticles and placed in a ٥٪ CO_2 incubator at ٣٧ °C for ٤٨ and ٧٢ hours. The culture medium containing iron oxide nanoparticles were discarded; the cells were washed three times with PBS, ٥ min each time. In the next step, the cells were fixed for ٢٠ minutes at ٣٧ °C with ٤٪ PFA; then, the washing steps were repeated. Cells by a ratio of ١:١ were incubated in media containing the ١ ml Potassium hexacyanoferrate (II) trihydrate ٤٪ ($K_4[Fe(CN)_6] \cdot 3H_2O$) and ١ ml HCL ١,٥٪ for ٢٠ min at room temperature, washed three times with warm PBS. Next, Safranin-O Staining was added to the wells (١ml per well) for ٥ minutes at room temperature. Finally, after three times of washing with warm PBS, the stem cells were assessed using invert microscopy.

Atomic Absorption Spectroscopy (AAS)

Cells were incubated at concentrations of ٠, ١٠٠, ٢٠٠, and ٣٠٠ µg/ml of iron oxide nanoparticles and placed in a ٥٪ CO_2 incubator at ٣٧ °C for ٤٨ and ٧٢ hours, twenty-four hours after transferring the stem cells to a flask. hEMSCs were harvested using the trypsin-EDTA solution, were washed three times with warm PBS, centrifuged, and were then diluted to ٠,٥ using PBS. In the following step, cells were boiled in ٩ cc HNO_3 (٣٢,٥٪). The amount of iron oxide emitted into the solution was measured by an atomic absorption spectrometer (Shimadzu, Japan)

MRI

Stem cells were incubated at concentrations of ٠, ١٠٠, ٢٠٠, and ٣٠٠ µg/ml of iron oxide nanoparticles and placed in a ٥٪ CO_2 incubator at ٣٧ °C for ٤٨ and ٧٢ hours, and also ٢٤ in ٦-well plates. hEMSCs were harvested using the trypsin-EDTA solution, washed three times with warm PBS, centrifuged, and were then diluted to ٠,٥ using PBS. Taurine was added to homogenize cells and then sonicated. Finally, MRI ١,٥ Tesla (Magnetom Avanto and Magnetom Aera, Siemens) was performed according to the following program: TE ranging from ١٣ ms to ١٣٢, TR of ٣٠٠٠ ms. fov=٢٣ cm, slice thickness=٨ mm, and acquisition matrix=٢٥٦×٢٥٦.

MTT Test

Cells were incubated at ٠, ١٠٠, ٢٠٠, and ٣٠٠ µg/ml of iron oxide nanoparticles. Next, culture medium containing iron oxide nanoparticles was changed and rinsed three times with PBS each for ٥ minutes.١٠ mg of tetrazolium powder dissolved in ٢ ccs of PBS and added ٢ µl to each well; after that, ١٥٠ µl was added to the wells, and placed in a CO_2 incubator at ٣٧ ° C for ٤-hours.١٠٠ µl DMSO was added. ١٠ minutes later, the plate was read at a wavelength of ٥٧٠ to ٦٣٠ nm by ELISA reader. The percentage of living cells

Table 1. List of primers' sequence used for RT-PCR

Name of genes	Forward primers' sequence	Reverse primers' sequence
BAX	CGCCCTTTTCTACTTTGACA	GTGACGAGGCTTGAGGAG
CASP3	GGACTGTGGCATTGAGAGAG	GGAGCCATCCTTTGAACTTC
BCL2	TGGTCTTCTTTGAGTTCGG	GGCTGTACAGTTCCACAA
BECLIN	GGGATGAGGGATGGAAGGGT	GGGGTGTGGTAAGTAATGGAG
LC3	GTGGTGGATGGTGGGATGGG	GTCTTTCAGGGGTGGGCAGGT
TP53	TTCCGTCTGGGCTTCTTG	TGCTGTGACTGCTTGTAGAT
GAPDH	GCAGGGATGATGTTCTGG	CTTTGGTATCGTGGAAGGAC

relative to the control absorption was then obtained. The test was repeated three times, and each concentration was repeated twice per test.

Oxidative Stress Assessment

Cells were incubated at concentrations of ٠, ١٠٠, ٢٠٠, and ٣٠٠ µg/ml of iron oxide nanoparticles and were placed in a ٥٪ CO٢ incubator at ٣٧ °C for ٤٨ and ٧٢ hours. After washing with ١x buffer, ٥٠ µl DCFDA solution (ab١١٣٨٥١ DCFDA Cellular ROS Detection Assay Kit), plates were kept in complete darkness for at least ٤٠ min, and were then washed with ١x buffer. Afterwards, light absorption was read by fluorimetry at a wavelength of ٤٨٥ and ٥٣٥nm. The test was repeated three times, and each concentration was repeated twice per test.

Lactate dehydrogenase assay (LDH)

Cells were incubated at concentrations of ٠, ١٠٠, ٢٠٠, and ٣٠٠ µg/ml of iron oxide nanoparticles and were placed in a ٥٪ CO٢ incubator at ٣٧°C for ٤٨ and ٧٢ hours. Then, the test of LDH assessment was performed based on protocol (LDH kit, Sigma, USA).

Gene Expression Assessments

To perform Real-Time PCR, RNA was extracted based on the manufacturer's instructions (Germany. QIAGEN) ٧٢ h after incubating stem cells at concentrations of ٠, ١٠٠, ٢٠٠, and ٣٠٠ µg/ml of iron oxide nanoparticles; they were placed in a ٥٪ CO٢ incubator at ٣٧°C. Following high-quality RNA extraction, cDNA was synthesized according to the manufacturer's instructions (Fermentas, USA) and was used to reverse transcription (Applied Biosystems) reaction using primers in Table ١. To prepare cDNA, a single-strand Oligo (dt) primer was presented (MWG-Biotech, Germany), and a reverse transcription enzyme (Fermentas, USA) was used. According to the manufacturer's instruction, PCR was carried out using PCR master mix (Applied Biosystems) SYBER Green using ABI Step One (Applied Biosystems, Sequences Detection Systems). Each Real-Time PCR cycle was run for ٤٠ cycles where each cycle was set to ٩٤°C for ٢٠ seconds, ٨٨-٨٠°C for ٣٠ seconds, and ٧٢°C for ٣٠ seconds. GAPDH gene was used as an internal control to normalize gene expression level.

Statistical analysis

Parametric variables were analyzed using one-way ANOVA (between three or more groups) followed by Scheffe and Tukey test. P-value less than ٠,٠٥ ($p < ٠,٠٥$) was considered statistically significant.

٣. Results

hEMSCs Isolation and proliferation

The spindle-shaped hEMSCs presented a fibroblast-like morphology which confirmed the correctness of our cell isolation (Figure ١A).

Flow Cytometry Analysis

Flow cytometry results confirm that the isolated cells do not express hematopoietic cell markers, whereas they show mesenchymal cell markers which is along with the morphology assessment (Figure ١B and C). The Flow cytometry was done for identifying hEMSCs, and the percentages of CD٤٥, CD٢٩, CD٩٠, CD٣٤, and CD١٠٥ markers are presented in (Figure ١E٣)

Alizarin Red staining: Osteogenic Differentiation Assessment

As shown in figure ١ D, due to calcium deposition, the differentiated cells in the bone turned red when stained with Alizarin Red. Bone nodules located in differentiated cells turned red color.

Oil Red-O staining: Adipogenic Differentiation Assessment

Differentiated areas turned red resulting in triglycerides reaction with red oil color. Adipocyte-containing fat droplets can be seen as red vacuoles accumulated within the cytoplasm (Figure ١ E).

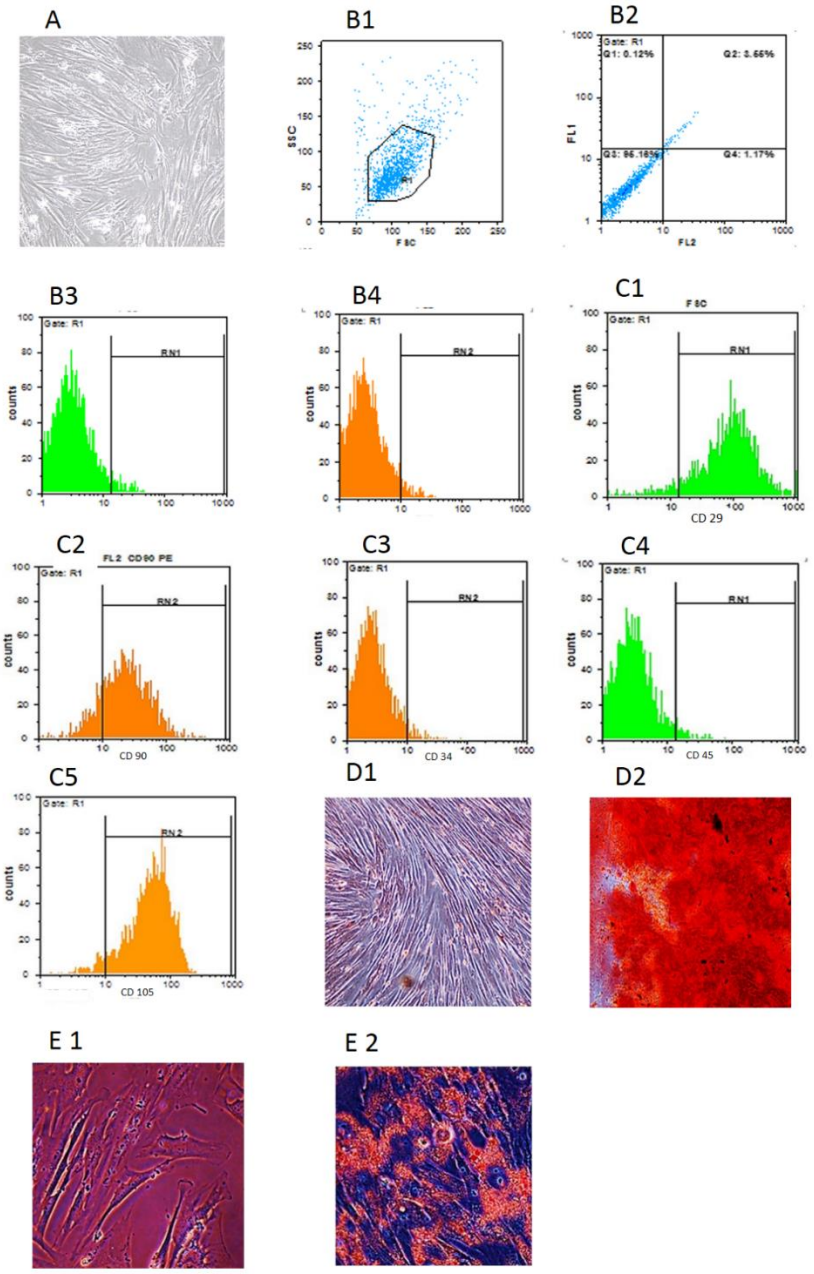

Figure 1. Characteristics of the mesenchymal stem cells. A) The first passage of stem cells isolated from endometrial (Magnificent 200). B) Flow cytometry analyses of third-passage of human endometrium-derived Mesenchymal stem cells. Cell response to isotype control. C) Flow cytometry analyses of third-passage of human endometrium-derived mesenchymal stem cells for; CD29, CD90, CD34, CD45, and CD105. D) Osteogenic differentiation (Magnificent 200); Cell matrix stained with Alizarin-Red and unstained cells. E) Adipogenic differentiation (Magnificent 200); Red fat vacuoles in response to Oil-Red-O staining and unstained cells. E3) percentage of CD45, CD29, CD90, CD34, and CD105 markers

hEMSCs incubation with iron oxide nanoparticles

As seen in figure ٢A, ٧٢ h after iron oxide nanoparticles incubation, the cells attached to the bottom of the flask while keeping their spindle morphology.

Prussian Blue Staining

PEG-coated SPION uptake into the cytoplasm of hEMSCs was confirmed by Prussian Blue staining ٤٨ and ٧٢h after incubation at ٠, ١٠٠, ٢٠٠, and ٣٠٠ µg/ml

concentrations (Figure ٢B).

Atomic Absorption Spectroscopy (AAS)

The data confirm that PEG-coated SPION absorption by hEMSCs was increasing with more doses (P<٠,٠٥) (Figure ٢C).

MRI: Evaluation of SPION Entrance into hEMSCs

As shown in Figure ٢ D, as the PEG-coated SPION concentration increased and longitudinal, transverse relaxation times in MRI images augmented, generating a signal darkening on MRI.

MTT test

MTT test results showed that at an optimum concentration of PEG-coated SPION, which was ١٠٠ µg/ml, cell viability was not significant compared to that of the control group. Furthermore, cell viability decreased over time and in a PEG-coated SPION dose-depended manner (Figure ٣A).

Oxidative Stress

Our result showed that ROS production significantly increased as the PEG-coated SPION concentration rose (Figure ٢B).

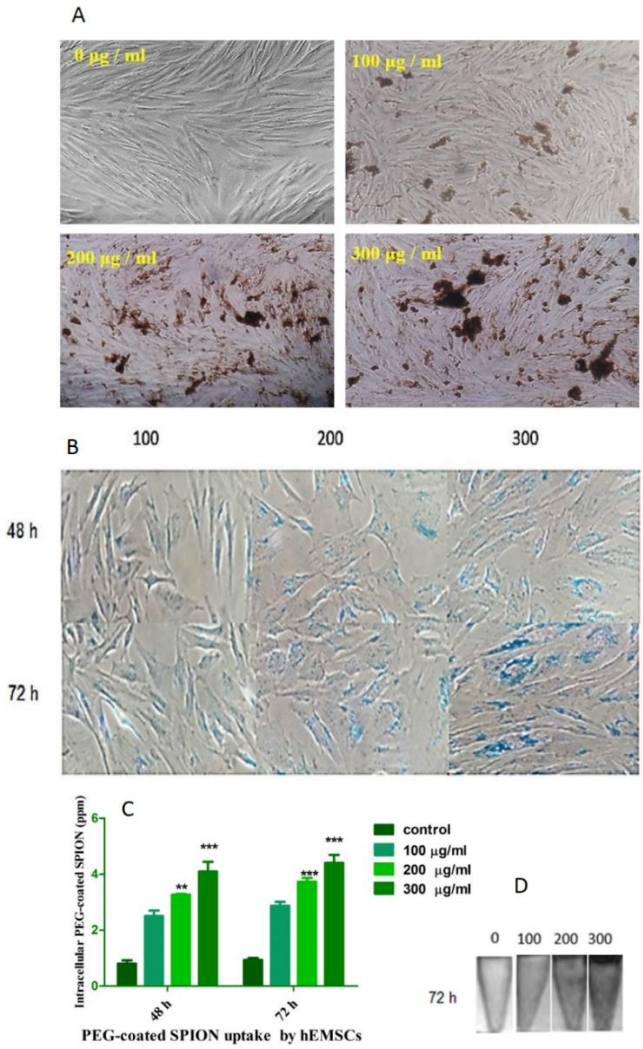

Figure 2. Evaluation of Cells morphology (Magnificent 200) 72h after PEG-coated SPION incubation at; 0, 100, 200, and ٣٠٠ µg/ml concentrations (A). Evaluation of PEG-coated SPION uptake into the cytoplasm of hEMSCs ٤٨ and ٧٢h after incubation at 100, 200 and 300 µg/ml concentration with Prussian Blue staining (Magnificent 400) (B). PEG-coated SPION uptake by hEMSCs 48 and 72h after incubation at 0,100,200, and 300 µg/ml concentrations (P<0.05). (**p< 0.0 ١, ***p< ٠,٠ ٠١ vs. Control). Data are presented as means ± S.E.M (C). MRI images of PEG-coated SPION-labeled hEMSCs at ٠,١٠٠,٢٠٠, and ٣٠٠ µg/ml concentrations of nanoparticle, ٧٢ h after incubation (D)

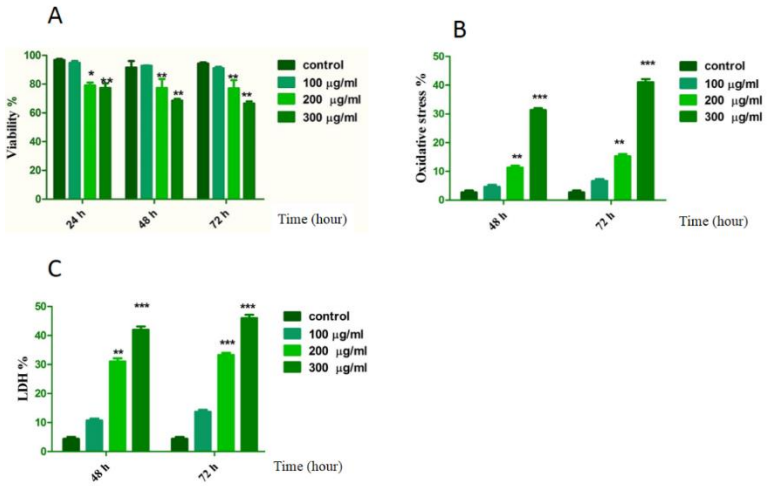

Figure 3. Evolution of cell survival in hEMSCS 24, 48 and 72h after incubation with PEG-coated SPION at 0, 100, 200, and 300 µg/ml concentrations. Data are presented as means ± S.E.M. A) MTT test (P<0.05). (*p< 0. 05 and **p< 0.01 vs. control). B) ROS production (P<0.05). (**p< 0. 01 and ***p< 0.0 01 vs. control). C) LDH release (P<0.05). (**p< 0. 01 and ***p< 0.0 01 vs. control)

Lactate dehydrogenase assay

According to our data, the most LDH release was seen at ٣٠٠ µg/mL PEG-coated SPION concentration ٧٢ after incubation (p<٠,٠٠٠). It means PEG-coated Spion caused to increase in LDH release into hEMSCs in a time and dose-dependent manner (Figure ٢C).

Apoptotic and Autophagy-associated markers

We evaluated the apoptotic and autophagy-associated markers using RT-PCR on hEMSCs labeled with PEG-coated SPION. BAX, CASP٣, and BCL٢ were evaluated as apoptotic pathway markers, while BECLIN, LC٣, and TP٥٣ were assessed as autophagy markers. GAPDH was used as the housekeeping gene.

As depicted in Figure ٤A, a significant increase in mRNA levels of pro-apoptotic markers, including Bax and Caspase٣, was observed as PEG-coated SPION concentration increased (P< ٠,٠٥). In contrast, mRNA levels of the anti-apoptotic marker, Bcl٢, markedly decreased in a dose-dependent manner, specifically at ٣٠٠ µg/ml concentration (P< ٠,٠٥). In addition, our results showed that there was a significant rise in mRNA levels of autophagy-associated markers such as BECLIN, LC٣, and TP٥٣ (P< ٠,٠٥) (Figure ٤B).

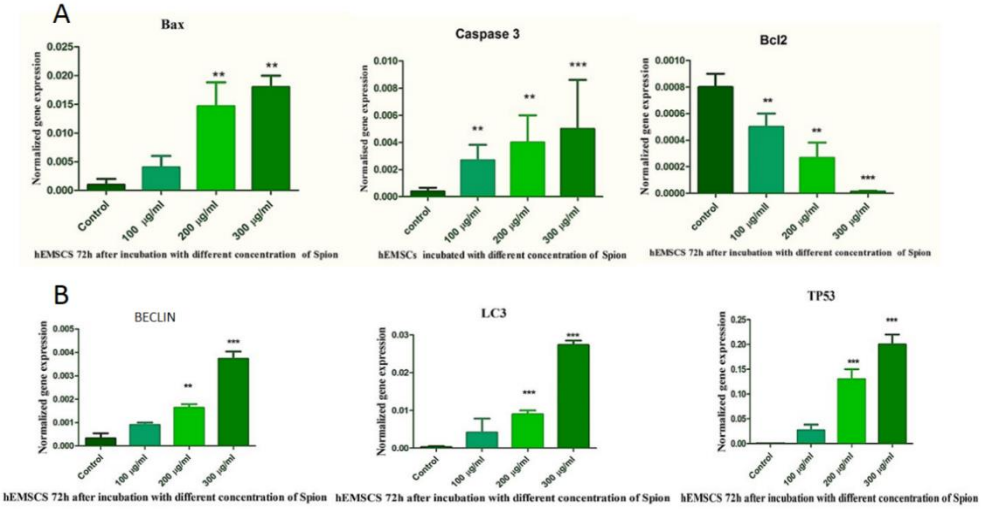

Figure ٤. mRNA levels of apoptotic associated-markers (A) and autophagy-associated markers (B) (**p< ٠. ٠١ and ***p< ٠,٠ ٠١ vs. Control). Data are presented as means ± S.E.M

٤. Discussion

The mesenchymal stem cell is one of the most important cells utilized for the treatment of different diseases such as neurological problems, diabetes, cardiac ischemia, and cartilage and bone disorders [١٧]. Thus, in this research, we isolated MCSs and performed three tests: Flow Cytometry and two different stainings, Alizarin-Red for checking the ability of these cells in osteogenic differentiation and Oil-Red-O for adipogenic differentiation. The results obtained from all of them confirmed the stemness of the isolated cells (Figure ١A-E). Because based on Flow Cytometry tests, the markers of mesenchymal stem cells such as CD٤٥, CD٢٩, CD٩٠, CD٣٤, and CD١٠٥ were expressed on the cell surface of isolated cells. The results of hEMSCs incubation with iron oxide nanoparticles showed the viability of hEMSCs after nanoparticle absorption (Figure ٢A). Hence, it can be a wise cell candidate.

After cell-transplantation, the cell tracing is the most critical stage. To track the fate of transplanted cells, various nanoparticles with different coatings have been used. The effects of nanoparticles on cell survival and their toxicity have remained a challenge in regenerative medicine. Ideal nanoparticles should be easily absorbed by cells without any cytotoxicity. In addition, they must stay in the cytoplasm for a long time because the long-term fate of transplanted cells should be monitored [١٨-٢٠]. The iron oxide nanoparticle holds all of these characteristics and is an FDA-approved biocompatible. As its amount is far less than the total body iron content, it is metabolized based on iron homeostatic mechanisms while not affecting oxidative stress balance. Moreover, they can move towards a magnetic field [٦, ٢١]. Based on this information and our previous work, we chose the PEG-coated SPION as our nanoparticles. To be sure that the PEG-coated SPION has been uptaken into the cytoplasm of hEMSCs Prussian Blue staining, Atomic Absorption Spectroscopy, and MRI were performed. The results of all the three tests confirmed the acceptable absorption of the PEG-coated SPION into the hEMSCs (Figure ٢B-D).

The mechanisms by which nanoparticles play their role in the body have not been fully understood yet. However, several studies have implicated that their excessive levels can cause reactive oxygen species (ROS) production in the plasma membrane and Mitochondria such as peroxides, superoxide, and hydroxyl radicals as well as apoptosis, inflammation, DNA damage, and reduced cell proliferation [٢٠-٢٤]. In our study, by MTT test, the optimum concentration of the PEG-coated SPION was determined (١٠٠ µg/ml) and ROS production and LDH release in hEMSCS showed a direct relationship between cell death and the dose of nanoparticles and time (Figure ٣A-C). Inconsistent with our results, it is confirmed that PEG-coated SPION-related cell damages occur in a dose-dependent manner. Hence, choosing the proper dose is crucial to avoid PEG-coated SPION cytotoxicity. Several studies have been done to assess the effects of different doses of nanoparticles with different coatings on the survival of various cell types. For example, a study of ١٥-nm dextran coated-iron oxide nanoparticles (٥٠ µg/ml) was incubated with human fibroblasts for three days. The results showed that at ٥٠ µg/ml concentration, nanoparticles reduced cell proliferation and led to cell death [٢٥, ٢٦]. Additionally, in another study, ١٥-nm dextran-coated-iron oxide nanoparticles (١٠٠ µg/ml) were incubated with human macrophages for seven days and only ٢٠٪ of the cells survived [٢٠]. In this study, fewer cells survived after ٢٤h, ٤٨h, and ٧٢h in comparison with those of the control, respectively. In agreement with our results, it was reported by several studies that nanoparticles associated with cell damage mainly in a dose and time-dependent manner [٢٧-٢٩].

In line with our study, some studies have investigated these nanoparticles to achieve a non-toxic dose, especially in the drug delivery area. For instance, Naqvi evaluated in vivo concentration-dependent toxicity of iron oxide nanoparticles on human macrophages and reported that the increased concentration of iron oxide nanoparticles led to a rise in ROS production, which caused cell damage and death [٢٧]. Another study reported that iron oxide nanoparticles entered into lysosomes by rupturing its membrane leading to the release of the lysosome's enzymes and cell damage [٣٠, ٣١]. In addition, it was shown that iron metabolism destroyed the surface of iron oxide nanoparticles and induced oxidative stress because of iron overload [٣٢]. Therefore, it seems that high doses of PEG-coated SPION give rise to oxidative stress and DNA damage, eventually causing cell necrosis and apoptosis [٣٣-٣٥].

Ansari et al. conducted a study to investigate in vivo and in vitro interaction of SPIONs with DNA and other toxic effects of the nanoparticles. The results showed that Iron oxide nanoparticles bind to nucleic acid bases and form a complex with DNA. On the other hand, these nanoparticles reduced cell survival by increasing lipid peroxidation and free radical production [٣٦]. Furthermore, in line with our results, Akter et al. showed that silver nanoparticles due to lipid peroxidation activated apoptotic signaling

pathways by damaging DNA [٣٧].

To evaluate the occurrence of apoptosis and autophagy, Real-Time PCR was performed for responsible genes. The results showed a significant up-regulation in pro-apoptotic markers including Bax, Caspase٣, BECLIN, LC٣, and TP٥٣ (P< ٠,٠٥), but down-regulation of the anti-apoptotic marker, Bcl٢ (P< ٠,٠٥) (Figure ٤A and B). As there is a complicated network in the cell, the exact reason for this down-regulation is not clear.

To sum up, our results confirm that when hEMSCs were incubated with PEG-coated SPION, free radical generation rose as the iron concentration increased; this finding is in agreement with that of our previous studies. In our previous study, we studied the absorption of PEG-coated SPION by stem cells isolated from the amniotic membrane and reported a satisfying absorption of this nanoparticle by mentioned cell and we determined the maximum non-toxic concentration, but not the exact mechanism of its toxicity. Thus, in this study, we focused on the mechanism of toxicity such as ROS production, autophagy, and apoptosis through gene expression evaluation while we know that the toxic dose not only depends on the kind of nanoparticle and its coating but also on cell type [١٩, ٢٠]. By comparing the results of these two studies, we concluded that as the tolerance of the human endometrial mesenchymal stem cells after ٧٢h was ١٠٠ µg/ml PEG-coated SPION, it is more sensitive to it in comparison with human amniotic membrane-derived mesenchymal stem cell which was ١٢٥ µg/ml after ٧٢h. In fact, these concentrations would be the non-toxic and therapeutic dose of PEG-coated SPION for incubating with these two cell types because, at these concentrations, toxicity was not statically significant in comparison with that of their control groups.

٥. Conclusion

In this investigation, the PEG-coated SPION was introduced for hEMSCs tracking for the first time; the mechanism of its toxicity in the higher concentrations was evaluated, and the threshold of the toxicity in the hEMSCs was found for the first time. In summary, higher concentrations of PEG-coated SPION improved MRI image contrast and enhanced cell fate tracking, but increased ROS production in a dose and time-dependent manner which initiates apoptosis, oxidative stress, and autophagy. Therefore, as the nontoxic doses of PEG-coated SPION are specific for each cell line, we suggest that before labeling each cell line with nanoparticles, their nontoxic doses be calculated accurately.

Ethical Considerations

Compliance with ethical guidelines

This investigation was approved by the Ethics Committee of the Iran University of medical science (Code: IR.IUMS.RC.١٣٩٩,٠٨٤).

Funding

This research was funded partly by the Iran University of medical science and partly by the author of this reserch article.

Author's contributions

Nahid Aboutaleb designed the study, Mahdieh Mehrab Mohseni wrote the article, Ghazal Yousefi did a part of the analysis, and Maryam Naseroleslami did most part of the study.

Conflict of interest

There is no conflict of interest.

Acknowledgments

The authors express their deepest gratitude to all participants whose biopsies were used in this study. This study has been financially supported by the Physiology Research Center of Iran University of Medical Sciences.

References

[1] Kalimuthu S, Oh JM, Gangadaran P, Zhu L, Lee HW, Rajendran RL, et al. In vivo tracking of chemokine receptor CXCR4-engineered mesenchymal stem cell migration by optical molecular imaging. Stem Cells Int. 2017; 2017:8085637. [DOI:10.1155/2017/8085637] [PMID] [PMCID]

[2] Malina T, Poláková K, Skopalík J, Milotová V, Holá K, Havrdová M, et al. Carbon dots for in vivo fluorescence imaging of adipose tissue-derived mesenchymal stromal cells. Carbon. 2019; 152:434-43. [DOI:10.1016/j.carbon.2019.05.061]

[3] Kheila M, Gorjipour F, Hosseini Gohari L, Sharifi M, Aboutaleb N. Human mesenchymal stem cells derived from amniotic membrane attenuate isoproterenol (ISO)-induced myocardial injury by targeting apoptosis. Med J Islam Repub Iran. 2021; 35:82. [DOI:10.47176/mjiri.35.82] [PMID] [PMCID]

[4] Kim JH, Lee HJ, Doo SH, Yang WJ, Choi D, Kim JH, et al. Use of nanoparticles to monitor human mesenchymal stem cells transplanted into penile cavernosum of rats with erectile dysfunction. Korean J Urol. 2015; 56(4):280-

٧. [DOI:١٠,٤١١١/kju.٢٠١٥,٥٦,٤,٢٨٠] [PMID] [PMCID]

[5] Santoso MR, Yang PC. Magnetic nanoparticles for targeting and imaging of stem cells in myocardial infarction. Stem Cells Int. 2016; 2016:4198790. [DOI:10.1155/2016/4198790] [PMID] [PMCID]

[6] Jasmin, de Souza GT, Louzada RA, Rosado-de-Castro PH, Mendez-Otero R, Campos de Carvalho AC. Tracking stem cells with superparamagnetic iron oxide nanoparticles: perspectives and considerations. Int J Nanomedicine. 2017; 12:779-93. [DOI:10.2147/ijn.s126530] [PMID] [PMCID]

[7] Naseroleslami M, Aboutaleb N, Parivar K. The effects of superparamagnetic iron oxide nanoparticles-labeled mesenchymal stem cells in the presence of a magnetic field on attenuation of injury after heart failure. Drug Deliv Transl Res. 2018; 8(5):1214-25. [DOI:10.1007/s13346-018-٠٥٦٧-٨] [PMID]

[8] Jazayeri MH, Amani H, Pourfatollah AA, Avan A, Ferns GA, Pazoki-Toroudi H. Enhanced detection sensitivity of prostate-specific antigen via PSA-conjugated gold nanoparticles based on localized surface plasmon resonance: GNP-coated anti-PSA/LSPR as a novel approach for the identification of prostate anomalies. Cancer Gene Ther. 2016; 23(10):365-9. [DOI:١٠,١٠٣٨/cgt.٢٠١٦,٤٢] [PMID]

[9] Elkhenany H, Abd Elkodous M, Ghoneim NI, Ahmed TA, Ahmed SM, Mohamed IK, et al. Comparison of different uncoated and starch-coated superparamagnetic iron oxide nanoparticles: Implications for stem cell tracking. Int J Biol Macromol. 2020; 143:763-74. [DOI:10.1016/j.ijbiomac.2019.10.031] [PMID]

[10] Van de Walle A, Perez JE, Abou-Hassan A, Hémadi M, Luciani N, Wilhelm C. Magnetic nanoparticles in regenerative medicine: what of their fate and impact in stem cells? Mater Today Nano . 2020; 11:100084. [DOI:10.1016/j.mtnano.2020.100084]

[11] Bull E, Madani SY, Sheth R, Seifalian A, Green M, Seifalian AM. Stem cell tracking using iron oxide nanoparticles. Int J Nanomedicine. 2014; 9:1641-53. [DOI:10.2147/ijn.s48979] [PMID] [PMCID]

[12] Nucci LP, Silva HR, Giampaoli V, Mamani JB, Nucci MP, Gamarra LF. Stem cells labeled with superparamagnetic iron oxide nanoparticles in a preclinical model of cerebral ischemia: a systematic review with meta-analysis. Stem Cell Res Ther. 2015; 6(1):27. [DOI:10.1186/s13287-015-0015-3] [PMID] [PMCID]

[13] Cores J, Caranasos TG, Cheng K. Magnetically Targeted Stem Cell Delivery for Regenerative Medicine. J Funct Biomater. 2015; ٦(٣):٥٢٦-٤٦. [DOI:١٠,٣٣٩٠/jfb٦٠٣٠٥٢٦] [PMID] [PMCID]

[14] Xue W, Liu Y, Zhang N, Yao Y, Ma P, Wen H, et al. Effects of core size and PEG coating layer of iron oxide nanoparticles on the distribution and metabolism in mice. Int J Nanomedicine. 2018; 13:5719. [DOI:10.2147/IJN.S165451] [PMID] [PMCID]

[15] Darzi S, Werkmeister JA, Deane JA, Gargett CE. Identification and characterization of human endometrial mesenchymal stem/stromal cells and their potential for cellular therapy. Stem Cells Transl Med. 2016; 5(9):1127-٣٢. [DOI:١٠,٥٩٦٦/sctm.٢٠١٥-٠١٩٠]

[16] Rungsiwiwut R, Virutamasen P, Pruksananonda K. Mesenchymal stem cells for restoring endometrial function: An infertility perspective. Reprod Med Biol. 2021; 20(1):13-9. [DOI:10.1002/rmb2.12339] [PMID] [PMCID]

[17] Hmadcha A, Martin-Montalvo A, Gauthier BR, Soria B, Capilla-Gonzalez V. Therapeutic Potential of Mesenchymal Stem Cells for Cancer Therapy. Front Bioeng Biotechnol. ٢٠٢٠; ٨:٤٣. [DOI:١٠,٣٣٨٩/fbioe.٢٠٢٠,٠٠٠٤٣] [PMID] [PMCID]

[18] Naseroleslami M, Parivar K, Khoei S, Aboutaleb N. Magnetic resonance imaging of human-derived amniotic membrane stem cells using PEGylated superparamagnetic iron oxide nanoparticles. Cell J. 2016; 18(3):332-9. [DOI:10.22074/cellj.2016.4560] [PMID] [PMCID]

[19] Feng Q, Liu Y, Huang J, Chen K, Huang J, Xiao K. Uptake, distribution, clearance, and toxicity of iron oxide nanoparticles with different sizes and coatings. Sci Rep. 2018; 8(1):2082. [DOI:10.1038/s41598-018-19628-z] [PMID] [PMCID]

[20] Patil RM, Thorat ND, Shete PB, Bedge PA, Gavde S, Joshi MG, et al. Comprehensive cytotoxicity studies of superparamagnetic iron oxide nanoparticles. Biochem Biophys Rep. 2018; 13:63-72. [DOI:10.1016/j.bbrep.2017.12.002] [PMID] [PMCID]

[21] Khalid MK, Asad M, Henrich-Noack P, Sokolov M, Hintz W, Grigartzik L, et al. Evaluation of toxicity and neural uptake in vitro and in vivo of superparamagnetic iron oxide nanoparticles. Int J Mol Sci. 2018; 19(9):2613. [DOI:10.3390/ijms19092613] [PMID] [PMCID]

[22] Naseroleslami M, Parivar K, Khoei S, Aboutaleb N. Optimal concentration of PEG-coated Fe3O4 nanoparticles for generation of reactive oxygen species in human-derived amniotic membrane stem cells. Adv Stud Biol. 2015; 7(8):377-88. [DOI:10.12988/asb.2015.5634]

[23] Wang L, Wang Z, Li X, Zhang Y, Yin M, Li J, et al. Deciphering active biocompatibility of iron oxide nanoparticles from their intrinsic antagonism. Nano Res. ٢٠١٨; ١١(٥):٢٧٤٦-٥٥. [DOI:١٠,١٠٠٧/s١٢٢٧٤-٠١٧-١٩٠٥-٨]

[24] Dulińska-Litewka J, Łazarczyk A, Hałubiec P, Szafrański O, Karnas K, Karewicz A. Superparamagnetic iron oxide nanoparticles-current and prospective medical applications. Materials. 2019; 12(4):617. [DOI:10.3390/ma12040617] [PMID] [PMCID]

[25] Oh N, Park JH. Endocytosis and exocytosis of nanoparticles in mammalian cells. Int J Nanomedicine. 2014; 9(1):51-63. [DOI:10.2147/ijn.s26592] [PMID] [PMCID]

[26] Sun X, Gamal M, Nold P, Said A, Chakraborty I, Pelaz B, et al. Tracking stem cells and macrophages with gold and iron oxide nanoparticles – The choice of the best suited particles. Appl Mater Today. 2019; 15:267-79. [DOI:10.1016/j.apmt.2018.12.006]

[27] Naqvi S, Samim M, Abdin M, Ahmed FJ, Maitra A,

Prashant C, et al. Concentration-dependent toxicity of iron oxide nanoparticles mediated by increased oxidative stress. Int J Nanomedicine. 2010; 5:983-9. [DOI:10.2147/ijn.s13244] [PMID] [PMCID]

[28] Yan B, Zhou H, Gardea-Torresdey JL. Bioactivity of engineered nanoparticles. Springer; 2017. [DOI:10.1007/978-981-10-5864-6]

[29] Fernández-Bertólez N, Costa C, Bessa MJ, Park M, Carriere M, Dussert F, et al. Assessment of oxidative damage induced by iron oxide nanoparticles on different nervous system cells. Mutat Res Genet Toxicol Environ Mutagen. 2019; 845:402989. [DOI:10.1016/j.mrgentox.2018.11.013] [PMID]

[30] Hoskins C, Cuschieri A, Wang L. The cytotoxicity of polycationic iron oxide nanoparticles: common endpoint assays and alternative approaches for improved understanding of cellular response mechanism. J Nanobiotechnology. 2012; 10:15. [DOI:10.1186/1477-3155-١٠-١٥] [PMID] [PMCID]

[31] Mosqueda-Flores RI, Bravo-Ramírez SD, Paulino-Gonzalez AD, Garcia-Contreras R. Iron Oxide Nanoparticles: Antibacterial and Cytotoxic Activity—A Systematic Review. Sensor Letters. 2020; 18(8):596-604. [DOI:10.1166/sl.2020.4253]

[32] Salimi M, Sarkar S, Fathi S, Alizadeh AM, Saber R, Moradi F, et al. Biodistribution, pharmacokinetics, and toxicity of dendrimer-coated iron oxide nanoparticles in BALB/c mice. Int J Nanomedicine. 2018; 13:1483. [DOI:10.2147/IJN.S157293] [PMID] [PMCID]

[33] Cortajarena AL, Ortega D, Ocampo SM, Gonzalez-García A, Couleaud P, Miranda R, et al. Engineering Iron Oxide Nanoparticles for Clinical Settings. Nanobiomedicine. ٢٠١٤; ١: ٢. [DOI:١٠,٥٧٧٢/٥٨٨٤١] [PMID] [PMCID]

[34] El-Boubbou K. Magnetic iron oxide nanoparticles as drug carriers: clinical relevance. Nanomedicine. 2018; ١٣(٨):٩٥٣-٧١. [DOI:١٠,٢٢١٧/nnm-٢٠١٧-٠٣٣٦] [PMID]

[35] Vakili-Ghartavol R, Momtazi-Borojeni AA, Vakili-Ghartavol Z, Aiyelabegan HT, Jaafari MR, Rezayat SM, et al. Toxicity assessment of superparamagnetic iron oxide nanoparticles in different tissues. Artif Cells Nanomed Biotechnol. 2020; 48(1):443-51. [DOI:10.1080/21691401.2019.1709855] [PMID]

[36] Ansari MO, Parveen N, Ahmad MF, Wani AL, Afrin S, Rahman Y, et al. Evaluation of DNA interaction, genotoxicity and oxidative stress induced by iron oxide nanoparticles both in vitro and in vivo: attenuation by thymoquinone. Sci Rep. 2019; 9(1):6912. [DOI:10.1038/s41598-019-43188-5] [PMID] [PMCID]

[37] Akter M, Sikder MT, Rahman MM, Ullah AA, Hossain KF, Banik S, et al. A systematic review on silver nanoparticles-induced cytotoxicity: Physicochemical properties and perspectives. J Adv Res. 2018;9:1-16. [DOI:10.1016/j.jare.2017.10.008] [PMID] [PMCID]